Electronic Supplementary Material (ESI) for Chemical Communications.

Functional Modulation of Cytochrome C upon Specific Binding to DNA Nanoribbons

Materials and Instruments

Horse heart Cyt C and general chemicals were purchased from Aladin and used without purification. All DNA oligodeoxynucleotides were purchased from Invitrogen (Shanghai, China) and used without further purification. All water was purified by a Milli-Q water purification system. UV-visible absroption spectrum and Cytochrome C redox potential were recorded on UV-2550 (Shimadzu,Japan). Fluorescence Spetroscopy were recorded on RF-5301pc (Shimadzu,Japan). Circular dichroic spectral were acquired from Applied Photophysics (Chirascan, Britai). Chromogenic substrate method was recorded on microplate reader. AFM images were obtained from MultiMode 8 AFM (Bruker, Inc.).

Preparation of DNA Nanoribbons

Successful folding for the DNR1 and DNR4 was observed at the following conditions: all the staple strands and the scaffold strand (in the molar ratio of 1:1) were mixed to a volume of 100 μL in 1 × TA/Mg^{2+} buffer consisting of 40 mM Tris (pH 7.4), 20 mM aceticacid, and 12.5 mM magnesium acetate, and subjecting the mixture to a thermal-annealing ramp that cooled from 90 ºC to 20 ºC over the course of 2 h. Successful folding for the DNR2 and DNR3 were observed at the following conditions: all the staple strands and the scaffold strand (in the molar ratio of 3:2) were mixed to a volume of 100 μL in 1 × TA/Mg^{2+}buffer, and thermal annealing by rapid heating to 90 ºC followed by slow cooling to 4 ºC over 24 h. Then the DNA nanoribbons was purified using Microcon centrifugal filter devices (100 kDa MWCO, 3000 g speed, 10 min, 3 times) followed by washing with the 1×TA/Mg^{2+} buffer to remove single stranded DNA after assembly. The concentration of the DNRs after purification (C_{after}) could be calculated from the absorbance of the DNR before and after the purification, A_{before} and A_{after} by the following equation:

$$C_{after} = \frac{A_{after}}{A_{before}} C_{before}$$

We use the concentration of one copy unit to represent the concentration of DNRs in this

report. The concentration of copy units before purification (C_{before}) was assumed equal to the scafford DNA concentration quantified by measuring OD260 with the extinction coefficient ε 260 calculated with IDT's OligoAnalyzer.

DNA tetrahedron was synthesized at the following conditions: equimolar quantities of four strands for the formation of the tetrahedrons were mixed in buffer (20 mM Tris, 50 mM $MgCl_2$, pH 8.0) at 95 ℃ and then cooled to 4 ℃.

Chromogenic Substrate Method

The chromogenic substrate method was used to determine the redox activity of Cyt C. Firstly Cyt C (0.1 μM) incubated with different concentrations of DNA nanostructures for 12 h at 25 °C. Then the solutions reacted with 5, 5'-Tetramethylbenzidine (TMB) at 37 °C for 15 min in 96-well plates with slight shake on the shaking table to achieve the purpose of well-mixing. Finally Adding 1 M H_2SO_4 to stop reaction, generated the yellow products, and the absorbance was monitored at 450 nm by microplate reader. The redox activity of Cyt C has been analyzed according to the following equation:

$$RRA = \frac{A_{\mathrm{CytC}}}{A_{\mathrm{CytC/DNR}}} \times 100\%$$

Here *RRA* indicated relative redox activity of Cyt C, $A_{\mathrm{Cyt\ C}}$ and $A_{\mathrm{Cyt\ C/DNR}}$ were the absorbance values of reaction product of Cyt C or Cyt C/DNR with TMB

Cytochrome c Redox Potential

Stock solutions of 100 mM ferrocyanide, ferricyanide, and dithionite in 1×TA/Mg^{2+} (pH 7.4) were made fresh prior to use and degassed by vacuum to remove oxygen. A stock solution of 1 mM cytochrome c in 1×TA/Mg^{2+} (pH 7.4) were prepared. The Cyt C/DNR1 complex was prepared by incubating Cyt C with DNR1(0.14 μM) at 4 °C for 12 h. Working solutions, all with identical cytochrome c concentrations, were prepared from 35 μL of the stock cytochrome c solution and 35 μL of the stock ferrocyanide, ferricyandie, and dithionite to complement to 350

μL by 1×TA/Mg^{2+} (pH 7.4). Then 1 μL ferricyanide/cytochrome c solution and ferricyanide/cytochrome c/DNR1 were added to the ferrocyanide/cytochrome c solution respectively. Absorbances at 550 nm were measured of all three solutions using ShimadzuUV-2550.

The collected data was analyzed as follows. The absorbance at 550 nm for each step was normalized to the change in absorbance from the fully reduced state (sample in dithionite normalized to 1.0) to the fully oxidized state (sample in ferricyanide normalized to 0.0) to determine the fraction of reduced (ferroCyt C) and oxidized (ferriCyt C) cytochrome c using the following equation: $Fract_{\text{ferroCyt C}}$ (fraction ferrocytochrome c) = $\frac{[\text{ferroCytC}]}{[\text{ferroCytC}]+[\text{ferriCytC}]}=$ $\frac{A_{\text{sample},550}-A_{\text{ferriCytC},550}}{A_{\text{ferroCytC},550}-A_{\text{ferriCytC},550}}$ and $Fract_{\text{ferriCytC}}$ = 1- $Fract_{\text{ferroCyt C}}$, where $A_{\text{ferriCytC},550}$ is the cytochrome c absorbance at 550 nm in the fully oxidized state (i.e., in ferricyanide) and $A_{\text{ferroCytC},550}$ is the cytochrome c absorbance at 550 nm in the fully reduced state (i.e., in dithionite) and $A_{\text{sample},550}$ is the cytochrome c absorbance in ferrocyanide after each aliquot of sample containing ferricyanide was added. And each step, $\log\frac{Fract_{\text{ferroCytC}}}{Fract_{\text{ferriCytC}}}$ was plotted against log $\frac{Fract_{\text{ferroCN}}}{Fract_{\text{ferriCN}}}$ along with a linear fit of the data, as shown in Fig. 1a of the main text. The *x* intercept is the $\log\frac{Fract_{\text{ferroCN}}}{Fract_{\text{ferriCN}}}$ that corresponds to when the $\log\frac{Fract_{\text{ferroCytC}}}{Fract_{\text{ferriCytC}}}$ is unity. The redox potential of the ferri-/ferrocyanide half-reaction at this point is equal to that of the midpoint redox potential of cytochrome c. It is given by the Nernst equation, where in this case E^o= 430 mV and $\log\frac{Fract_{\text{ferroCN}}}{Fract_{\text{ferriCN}}}$ is the *x* intercept of Fig. 1a:

$$E = E^0 - 2.303\frac{RT}{nF}\log\left(\frac{[\text{ferroCN}]}{[\text{ferriCN}]}\right)$$

In this formula, *R* is the ideal gas constant of 8.314 $\frac{J}{mol*k}$, *T* is the temperature of the experiment in kelvin, *n* is one for the number of electrons involved in the oxidation-reduction

reaction, F is Faraday's constant of 96485 $\frac{C}{mol}$.

Cyt C Peroxidase Activity

The Cyt C peroxidase activity assays were performed in 750 μL quartz cuvettes by mixing 50 μL of 0-1200 mM guaiacol, 50 μL of 9100 mM H_2O_2, 200 μL 1×TA/Mg^{2+}, and 50 μL of ①Cyt C(70 μM), ②Cyt C(70 μM)/CL(210 mM), ③Cyt C(70 μM)/DNR1(0.7 mM), ④Cyt C(70 μM) /CL(210 mM)/DNR1(0.7 mM), ⑤Cyt C(70 μM)/CL(210 mM)/DNR1 mixtures(0.7 mM). The incubation solution was mixed for 14 h at 4 °C. The Cyt C/CL/DNR1 complexes were prepared when CL and Cyt C were incubated about 10 h and then added DNR1. The experiment could be monitored through absorbance at 470 nm .

The enzyme-activity data measured at different concentrations of substrates were used for nonlinear regrassion by Michaelis-Menten equation,:

$$V = (V_{max}[S])(K_m + [S]) = k_{cat}[E_t][S] / K_m + [S]$$

In this equation, K_m is Michaelis constant, k_{cat} is turnover number, [S] is concentration of substrate, $[E_t]$ is enzyme concentration.

K_D Experiments

A stock solution of 1 mM Cyt C in 1×TA/Mg^{2+} (pH 7.4) were prepared. 35 μL of the stock Cyt C solution was diluted to 350 μL by 1×TA/Mg^{2+} (pH 7.4). Then 5 μL DNR1(10μM) solution were added to the Cyt C solution six times. Absorbances at 408 nm were measured of the working solutions using ShimadzuUV-2550. The collected data was analyzed as following equation.

$$1/(A_0 - A) = 1/A_0 + 1/(K_D A_0 [DNR1])$$

A_0, A are the UV absorption values of the working solutions before and after the addition of DNR1 at 408 nm. Plot $1/(A_0\text{-}A)$ to 1/[DNR1], the ratio of intercept to slope is the binding constant K_D.

AFM Characterization

Samples were prepared by deposition of 2 μL onto freshly cleaved mica, and left to adsorb to the surface for 2 min. They were scanned in tapping mode on a MultiMode 8 AFM with NanoScope V Controller (Bruker, Inc.).

Native Polyacrylamide Gel Electrophoresis Analysis

For the native polyacrylamide electrophoresis experiment, DNR1 (2μM) was incubated with 300 μM Cyt C in 1×TA/Mg^{2+} buffer at 25 °C for 12 h, and all the samples were analyzed by 15% native polyacrylamide electrophoresis for 120 minutes at 4 °C at a constant 80 V in 1×TA/Mg^{2+}. The native polyacrylamide gel was soaked in a SYBR green solution to illuminate the DNA nanoribbons after completion of the electrophoresis, and then the same gel was stained in Coomassie Blue to identify the existence of the Cyt C.

UV-visible Absorption Spectrum

A UV-Vis spectrophotometer(Shimadzu,Japan) recorded the absorption spectrum of DNR1 (0.025 μM), Cyt C (3 μM) and Cyt C (3 μM)/DNR1(0.025 μM) complex. And incubation of Cyt C and DNR1 maintain for 12 h at 25 °C in 1×TA/Mg^{2+} buffer.

Fluorescence Spetroscopy

The fluorescence emission spectra were recorded in the presence of varying concentrations of DNR1 (from 0 to 0.09 μM). The fluorescence intensity was determined by exciting the sample solution at 430 nm. The excitation and emission slits were both maintained at 5.0 nm. The experiment was conducted at room temperature (25 °C) in a buffer containing 1×TA/Mg^{2+} (pH 7.4).

Synchronous Fluorescence Spectroscopy

The synchronous fluorescence measurements of Cyt C (5 μM) in the presence of varying concentrations of DNR1 were recorded. The excitation and emission slit width both were fixed at 5 nm. A constant wavelength interval of Δλ=20 nm or Δλ=80 nm was fixed to reveal the microenvironmental changes of tyrosine (Tyr) and tryptophan (Trp) residues, respectively.

Circular Dichroic Spectral

We obtained the circular dichroic spectra through a circular dichroism spectroscopy(Chirascan), from the British Photo Physics Company. Each sample solution with a total volume of 350 μL was scanned in the range of 200 nm-500 nm at 25 ℃, and the CD spectra was generated from which the buffer background had been subtracted.

DNA Sequence

Table S1 Oligonucleotide sequences used in this work

DNR1-S1	5'-CAG GGC TGG GCA TAG AAG TCA GGG CAG AGA CGA GTT GAG AAT ACG AGT TGA GAA GAG TAC TTG AGA ATC CGA CCA TTG TGC GCT ATC TTC ATC TTA-3'
DNR1-ST1	5'-CAG CCC TGT AAG ATG AAG ATA GCG TCT ATG CC-3'
DNR1-ST2	5'-CCC TGA CTC ACA ATG GTC GGA TTC CGT CTC TG-3'
DNR1-ST3	5'-TCT CAA CTT CAA CTC GTA TTC TCA ACT CGT AT-3'
DNR2-S1	5'-CAG GGC TGG GCA TAG AAG TCA GGG CAG AGA CGG AAT CCG ACC ATT GTG CGC TAT CTT CAT CTT A-3'
DNR2-ST1	5'-CAG CCC TGT AAG ATG AAG ATA GCG TCT ATG CC-3'
DNR2-ST2	5'-CCC TGA CTC ACA ATG GTC GGA TTC CGT CTC TG-3'
DNR3-S1	5'-CAG GGC TGG ACA TAG AAG TCA GAT CAG AGA CGA CTT GAG AAT AGG ATT CGA GTA TAT GCG TAC CTT GTC CGA CCA TTG TG-3'
DNR3-S2	5'-CCA ATC AAT CCG TCC TGT CAG ACC TGC GAA TGT GCC CAT CCG ATA ATC GGT CAT GGT GAA GCT GCC AGT CCC AAG AGT TA-3'
DNR3-ST1	5'-CAG CCC TGT AAC TCT TGG GAC TGG TCT ATG TC-3'
DNR3-ST2	5'-ATC TGA CTC AGC TTC ACC ATG ACC CGT CTC TG-3'
DNR3-ST3	5'-TCT CAA GTG ATT ATC GGA TGG GCA AAT CCT AT-3'
DNR3-ST4	5'-TAT ACT CGC ATT CGC AGG TCT GAC GGT ACG CA-3'
DNR3-ST5	5'-TCG GAC AAA GGA CGG ATT GAT TGG CAC AAT GG-3'
DNR4-S1	5'-CTC CTA ACT GTT CTA AGA GTC GAG CTG AAC CGT GGA CGA GGG ACC AGA CCC CGG AAG TAA TGA CAA GCA TGA ATG GTA CTA AGT GAG CGA GTG CTG-3'
DNR4-ST1	5'-GTT AGG AGC AGC ACT CGC TCA CTT TTA GAA CA-3'
DNR4-ST2	5'-CTC GAC TCA GTA CCA TTC ATG CTT CGG TTC AG-3'
DNR4-ST3	5'-CTC GTC CAG TCA TTA CTT CCG GGG TCT GGT CC-3'
tetrahedron-1	5'-GAG CGT TAG CCA CAC ACA CAG TC-3'
tetrahedron-2	5'-TTA GGC GAG TGT GGC AGA GGT GT-3'
tetrahedron-3	5'-CGC CTA AAC AAG TGG AGA CTG TG-3'
tetrahedron-4	5'-AAC GCT CAC CAC TTG AAC ACC TC-3'
DNR1-S1-1	5'-CAG GGC TGG GCA TAG AAG TCA GGG CAG AGA CGA GTT GAG AAT ACG AGT-3'
DNR1-S1-1*	5'-GTC CCG ACC CGT ATC TTC AGT CCC GTC TCT GCT CAA CTC TTA TGC TCA-3''
DNR1-S1-2	5'-TGA GAA TAC GAG TTG AGA ATC CGA CCA TTG TGC GCT ATC TTC ATC TTA-3'
DNR1-S1-2*	5'-ACT CTT ATG CTC AAC TCT TAG GCT GGT AAC ACG CGA TAG AAG TAG AAT-3'
DNR2-S1-1	5'-CAG GGC TGG GCA TAG AAG TCA GGG CAG AGA CG-3'

DNR2-S1-1*	5'-GTC CCG ACC CGT ATC TTC AGT CCC GTC TCT GC-3'
DNR2-S1-2	5'-GAA TCC GAC CAT TGT GCG CTA TCT TCA TCT TA-3'
DNR2-S1-2*	5'-CTTAGGCTGGTAACACGCGATAGAAGTAGAAT-3'
DNR3-S1	5'-CAG GGC TGG ACA TAG AAG TCA GAT CAG AGA CGA CTT GAG AAT AGG ATT CGA GTA TAT GCG TAC CTT GTC CGA CCA TTG TG-3'
DNR3-S1*	5'-GTCCCGACCTGAATCTTCAGTCTAGTCTCTGCTGAACTCTTATCCTA AGCTCATATACGCTAGGAACAGGCTGGTAACAC-3'
DNR3-S2	5'-CCA ATC AAT CCG TCC TGT CAG ACC TGC GAA TGT GCC CAT CCG ATA ATC GGT CAT GGT GAA GCT GCC AGT CCC AAG AGT TA-3'
DNR3-S2*	5'-GGTTAGTTAGGCAGGACAGTCTGGACGCTTACACGGGTAGGCTATT AGCCAGTACCACTTCGACGGTCAGGGTTCTCAAT-3'
DNR4-S1-1	5'-CTC CTA ACT GTT CTA AGA GTC GAG CTG AAC CGT GGA CGA GGG ACC AGA-3'
DNR4-S1-1*	5'-GAG GAT TGA CAA GAT TCT CAG CTC GAC TTG GCA CCT GCT CCC TGG TCT-3'
DNR4-S1-2	5'-CCC CGG AAG TAA TGA CAA GCA TGA ATG GTA CTA AGT GAG CGA GTG CTG-3'
DNR4-S1-2*	5'-GGG GCC TTC ATT ACT GTT CGT ACT TAC CAT GAT TCA CTC GCT CAC GAC-3'
1	5'-GAGCGTT-3'
1*	5'-CTCGCAA-3'
2	5'-GCCACAC-3'
2*	5'-CGGTGTG-3'
3	5'-GTGTCAG-3'
3*	5'-CACAGTC-3'
4	5'-AATCCGC-3'
4*	5'-TTAGGCG-3'
5	5'-GAGGTGT-3'
5*	5'-CTCCACA-3'
6	5'-CAAGTGG-3'
6*	5'-GTTCACC-3'

Design of DNA Nanoribbon

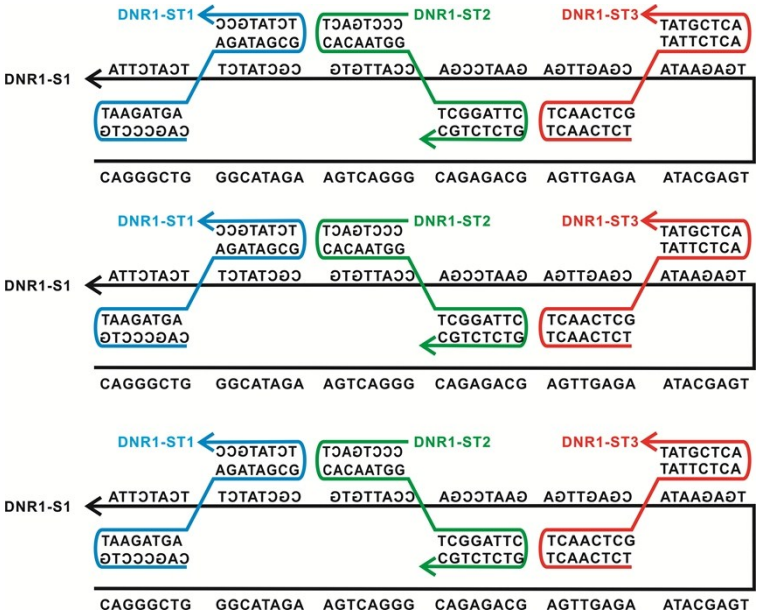

Fig. S1 Schematic illustration of the folding pathway of DNR1.

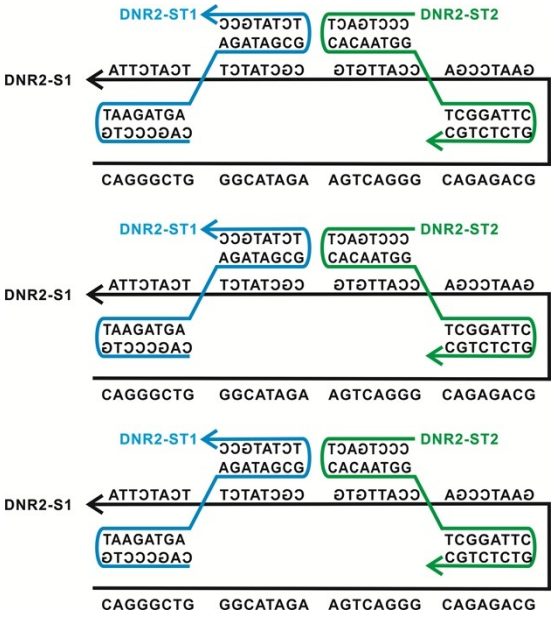

Fig. S2 Schematic illustration of the folding pathway of DNR2.

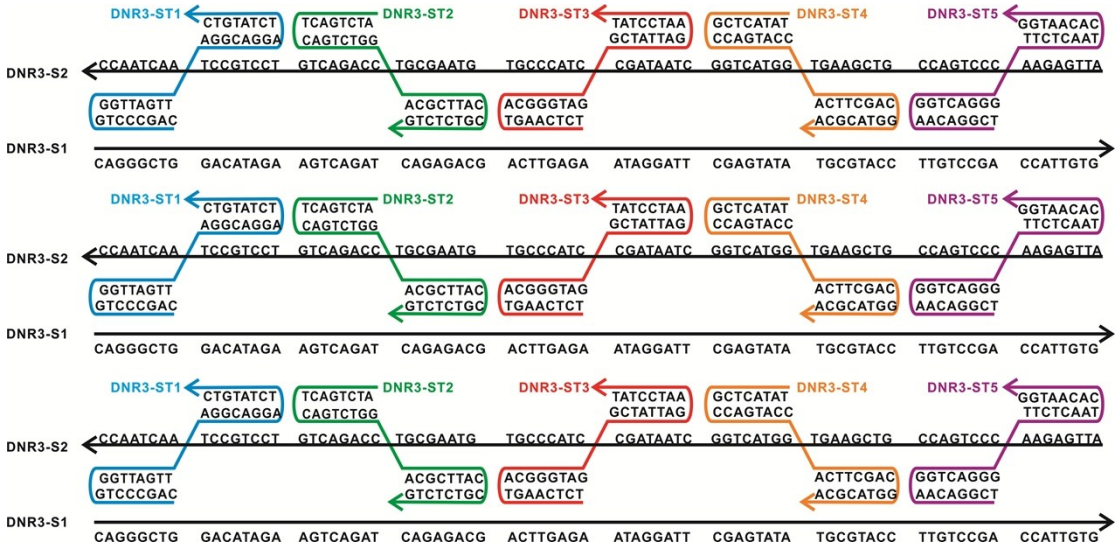

Fig. S3 Schematic illustration of the folding pathway of DNR3.

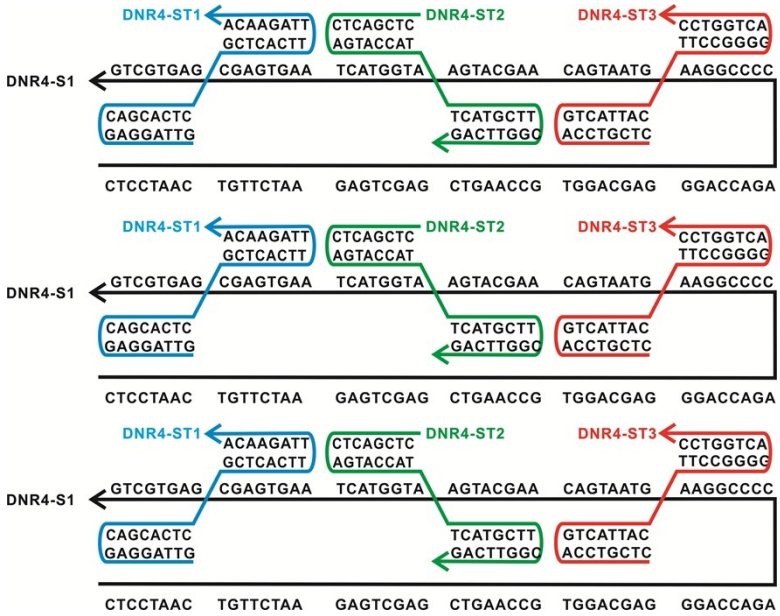

Fig. S4 Schematic illustration of the folding pathway of DNR4.

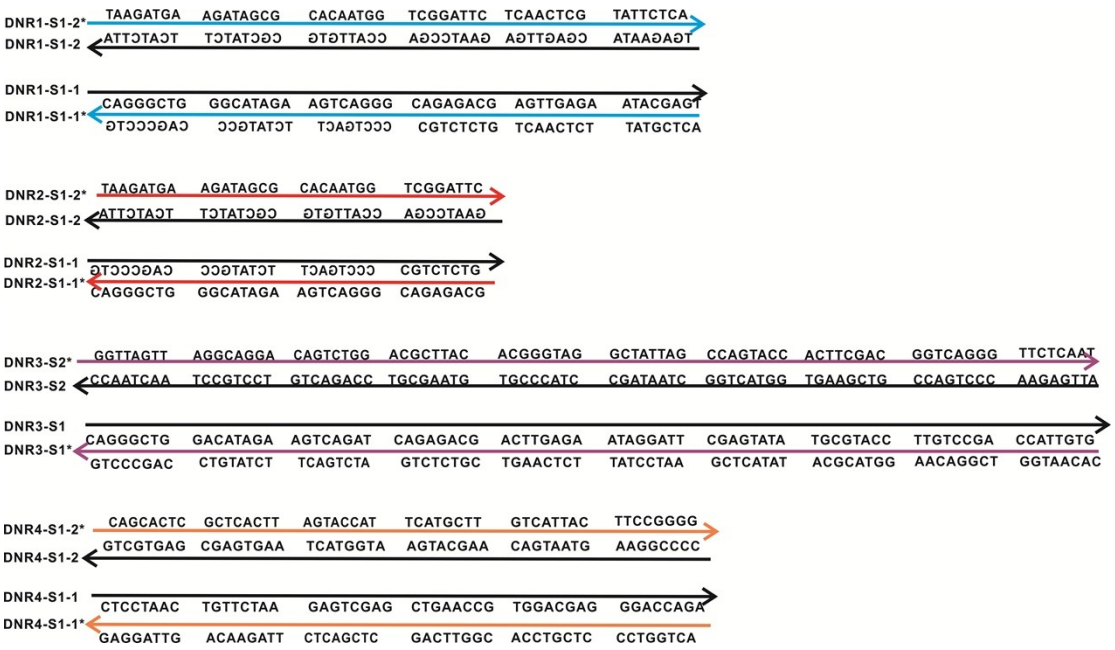

Fig. S5 Schematic illustration of double stranded control experiments of DNR1-4.

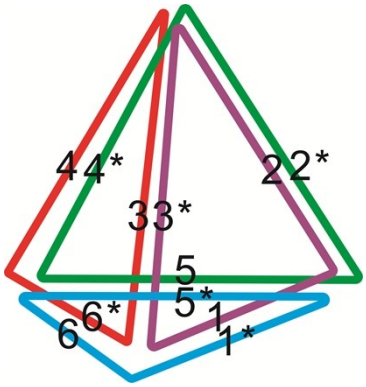

Fig. S6 Schematic illustration of double stranded control experiments of tetrahedron.

Supplementary Results

Table S2 Relative redox activity of Cyt C evaluated by the chromogenic substrate method. *

Structure / Concentration	DNR1	DNR1 ssMix[a]	DNR1 dsMix[b]	DNR2	DNR2 ssMix	DNR2 dsMix	DNR3	DNR3 ssMix	DNR3 dsMix	DNR4	DNR4 ssMix	DNR4 dsMix	Tetra[c]	Tetra ssMix	Tetra dsMix
0.0002 μM	107.68%	101.19%	102.89%	98.85%	103.37%	100.76%	98.57%	110.23%	101.65%	94.40%	101.16%	104.93%	99.20%	107.39%	103.11%
0.0004 μM	111.69%	102.30%	100.22%	101.15%	100.60%	101.13%	102.87%	99.59%	100.62%	100.58%	95.78%	101.00%	101.60%	105.93%	102.56%
0.0007 μM	125.80%	104.74%	100.43%	102.59%	101.29%	100.43%	103.15%	106.39%	101.98%	104.97%	96.65%	102.53%	102.13%	106.00%	102.55%
0.0009 μM	132.34%	107.25%	100.78%	102.31%	104.80%	101.25%	104.87%	108.19%	99.66%	105.85%	105.68%	99.27%	103.20%	106.58%	100.02%
0.0010 μM	135.91%	107.91%	100.86%	104.61%	100.28%	99.95%	107.74%	103.94%	101.48%	108.48%	108.47%	99.73%	107.98%	103.45%	104.72%
0.0020 μM	137.36%	112.69%	100.77%	105.76%	98.826%	102.05%	106.59%	91.63%	101.37%	110.82%	100.53%	99.07%	108.25%	105.11%	100.51%
0.0030 μM	141.88%	112.56%	100.17%	109.80%	98.83%	99.56%	112.26%	98.45%	101.33%	115.50%	107.12%	99.67%	109.84%	101.59%	105.12%
0.0040 μM	147.66%	118.21%	101.48%	114.12%	102.20%	102.00%	114.26%	101.45%	102.23%	122.22%	105.28%	102.32%	109.31%	92.54%	104.46%
0.0050 μM	157.62%	115.99%	102.75%	117.00%	98.19%	101.27%	119.27%	94.83%	101.26%	133.53%	103.04%	102.55%	114.36%	99.58%	103.48%
0.0060 μM	157.19%	121.51%	104.85%	137.37%	97.57%	101.62%	122.35%	89.85%	103.09%	133.33%	103.37%	101.90%	115.69%	113.11%	102.01%
0.0070 μM	162.60%	121.51%	101.54%	137.47%	104.09%	102.24%	120.63%	99.76%	103.13%	137.43%	100.10%	104.07%	113.03%	103.47%	101.50%
0.0080 μM	162.01%	122.94%	103.60%	136.60%	107.14%	101.16%	129.80%	99.68%	103.11%	138.01%	111.76%	99.92%	118.35%	101.87%	102.96%
0.0090 μM	171.66%	124.51%	101.14%	147.26%	103.78%	101.46%	148.14%	101.45%	103.02%	147.66%	123.74%	99.78%	119.95%	89.41%	104.17%
0.0100 μM	172.99%	130.33%	105.38%	142.30%	98.71%	102.21%	147.00%	103.98%	103.64%	148.25%	92.05%	101.26%	120.48%	109.04%	108.75%

*Substrate used: 3, 3', 5, 5'-Tetramethylbenzidine (TMB). The Cyt C without any additions was set as the 100% activity. It took an average of at least three independent experiments to obtain the Table S2. (a: ssMix means single-stranded mixture; b: dsMix means double-stranded mixture; c: Tetra means tetrahedron.)

Table S3 Kinetics and dissociation constants for Cyt C in different cases. Experimental conditions: 10 μM Cyt C, 40.0 mM Tris, 12.5 mM Mg^{2+}, pH 7.4. The temperature was 25 ºC. Standard deviations were averaged from at least three independent experiments.

Protein	k_{cat} (s^{-1}) (×10^{-1})	K_m (M) (×10^{-3})	k_{cat}/K_m (M^{-1} s^{-1})	K_D (μM)
Cyt C	5.6 (±0.4)	28.6 (±4.0)	19.9 (±3.2)	——
+ CL	6.2 (±0.4)	23.3 (±5.8)	28.1 (±8.7)	——
+ DNR1	5.1 (±0.5)	39.8 (±4.4)	13.0 (±2.7)	0.85（±0.14）
+ CL+ DNR1	5.9 (±0.2)	27.7 (±3.5)	21.6 (±3.5)	——
+ DNR1 ssMix	5.1 (±0.3)	29.9 (±0.3)	17.7 (±0.1)	1.2（±0.31）
+ DNR1 dsMix	6.3（±0.1）	30.4（±0.7）	20.8（±1.0）	1.76（±0.16）

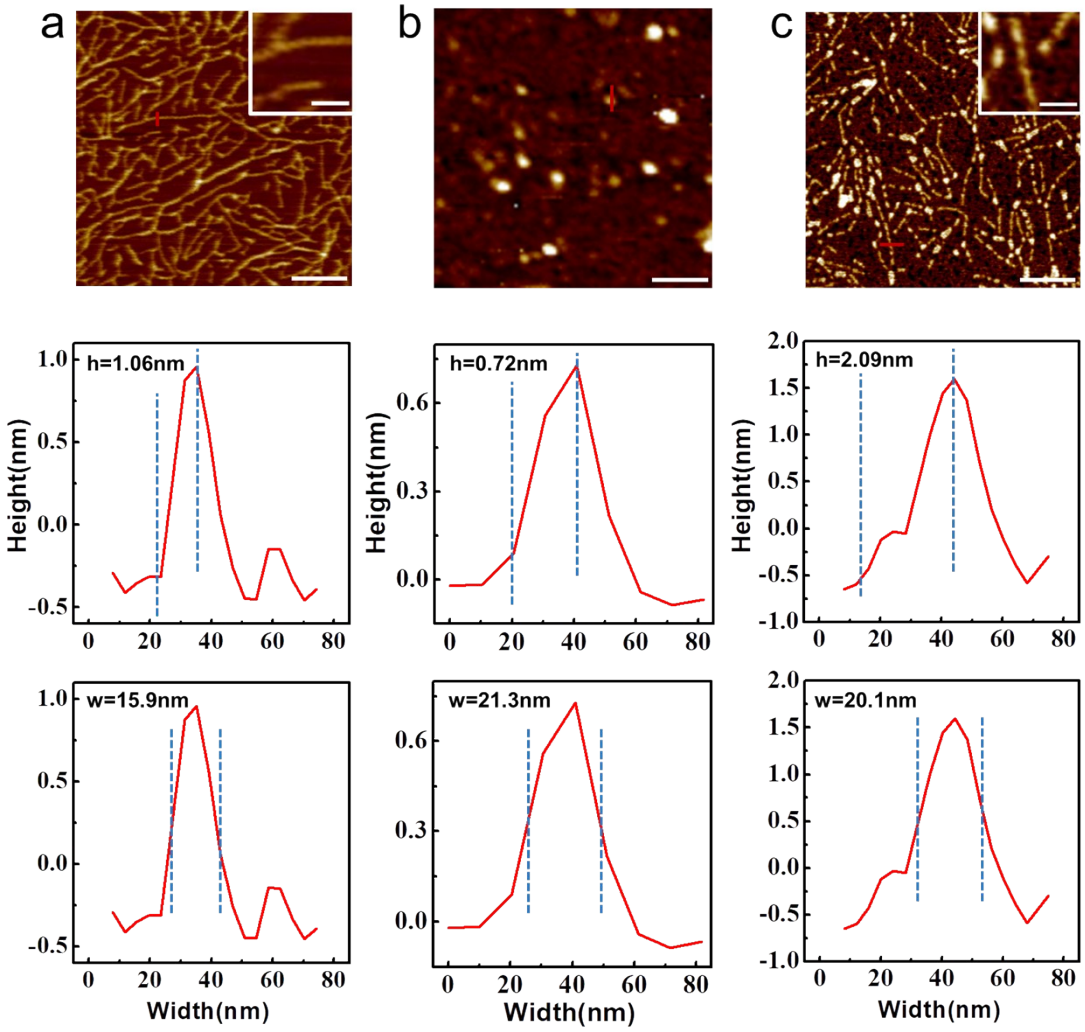

Fig. S7 AFM images of DNR1 (a), Cyt C (b) and Cyt C/DNR1 complex (c) with a zoom in image. Zoom out images with scale bars at 200 nm, and zoom in images with scale bars at 100 nm.

Fig. S7a and Fig. S7b shows that the width and height of DNR1 are 15.9 and 1.06 nm, respectively. Cyt C was present as a multimer in the solution with a width and height of 21.3 and 0.72 nm, respectively. The figure in the upper right corner of Fig. S7c clearly shows that Cyt C is distributed on the DNR1 at discrete points and the width and height of the Cyt C/DNR1 complex were 20.1 and 2.09 nm, respectively, indicating that the molecular size and morphology changed greatly after Cyt C was combined with DNR1.

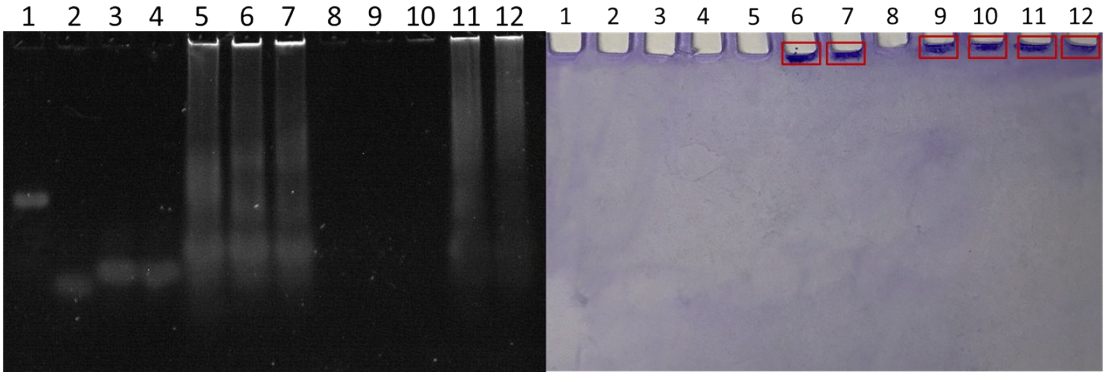

Fig. S8 Native polyacrylamide gel electrophoresis analysis. On the left, the 15% native polyacrylamide gel was stained by SYBR® Gold nucleic acid gel stain. On the right, the gel was stained by Coomassie Brilliant Blue R250. [DNR1] = 2 μM, [Cyt C] = 300 μM, [CL] = 600 μM. (Lane 1: DNR1-S1; Lane 2: DNR1-ST1; Lane 3: DNR1-ST2; Lane 4: DNR1-ST3; Lane 5: DNR1; Lane 6,Lane 7: Cyt C/DNR1 complex; Lane 8: Cyt C; Lane 9,Lane 10: Cyt C/CL complex; Lane 11,Lane 12: Cyt C/CL/DNR1 complex).

Fig. S8 is an image of native polyacrylamide gel electrophoresis. Lane 8 in the image on the right is Cyt C. Since Cyt C is positively charged in neutral buffer solution, no bands are present in lane 8. Lane 5 and lane 6,7 on the left are a comparison of free DNR1 and Cyt C/DNR1 complex. It can be seen that due to the combination of DNR1 and Cyt C, more DNR1 remains in the pores in the lane 6,7, at the same time, the blue band in the red square can be seen in the right lane 6, 7, indicating that the electrostatic interaction is not the only factor for DNR1 binding to Cyt C. In lane 9 and 10 on the right side is a complex of Cyt C and CL. Since CL is also negatively charged and not only electrostatically bonded to Cyt C, the blue band in the red square can also be seen. In lane 11 and 12 on the right side, there is a complex of Cyt C, CL and DNR1. For the same reason, the blue band in the red square can also be seen.

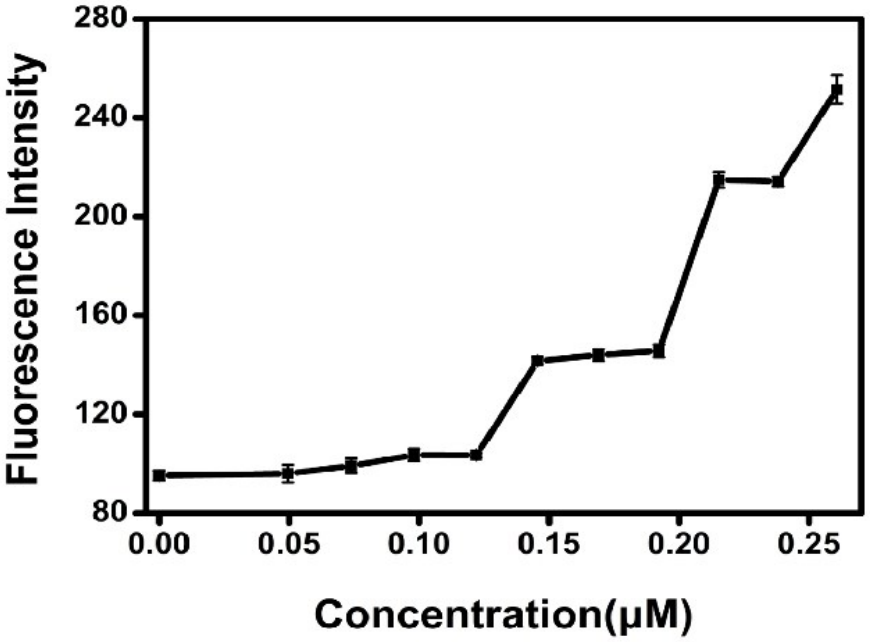

Fig. S9 Fluorescence intensity dependence on the concentration of DNR1. (Δλ=20nm)

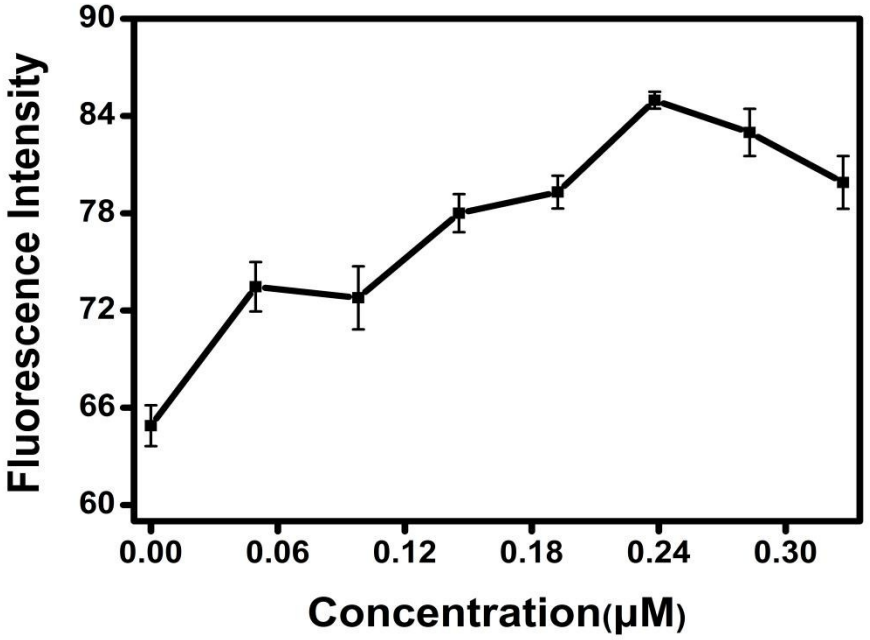

Fig. S10 Fluorescence intensity dependence on the concentration of DNR1. (Δλ=80nm)

Fig. S9 and Fig. S10 show the intensity dependence on the concentration for a 300-nm peak of tyrosine and a 380-nm peak of tryptophan, respectively. The results are similar to that obtained by dilution of the solution, which imply that DNR1 may disrupt energy transfer from the tyrosine and tryptophan residues to the heme group, the charged carboxy and/or amino groups in the cytochrome c molecule to prevent dynamic quenching during diffusion of Cyt C.

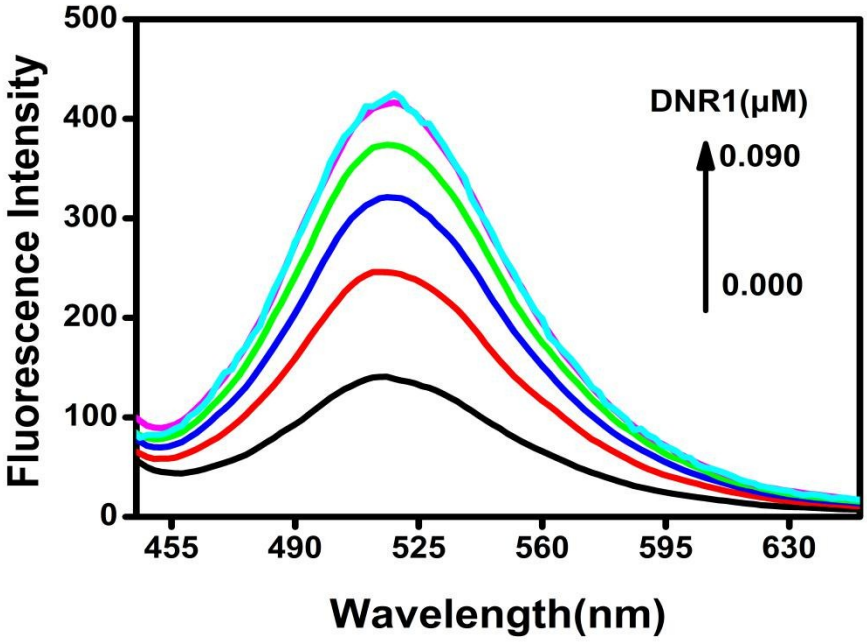

Fig. S11 Fluorescence emission spectra of Cyt C (5 μM) at different concentrations of DNR1 (from 0 to 0.09 μM)

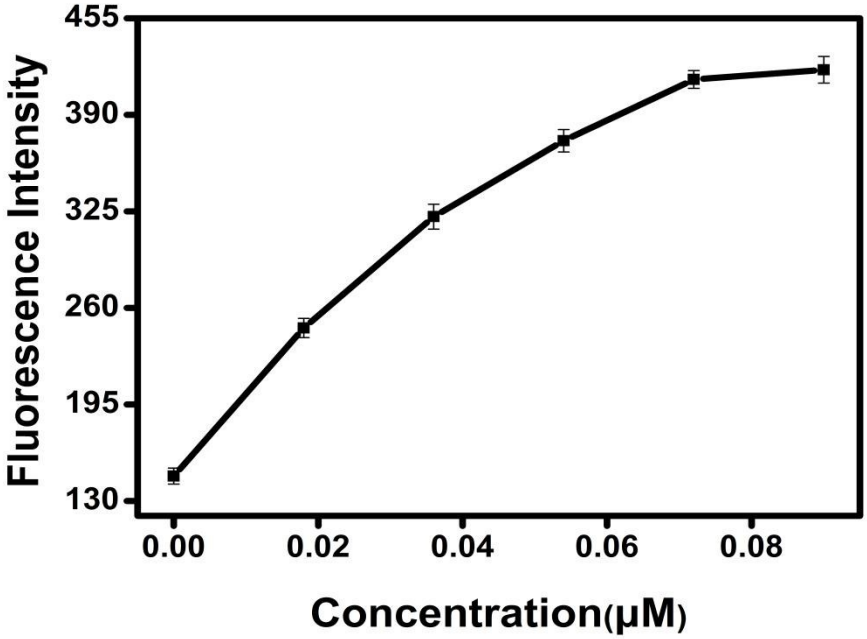

Fig. S12 Fluorescence intensity dependence on the concentration of DNR1 for 514 nm peak.

Fig. S11 and Fig. S12 show that the fluorescence intensity of Cyt C increased without changing the emission wavelength and the peak shape with the increasing of DNR1 concentration, which suggested that DNR1 can change microenviroment near the heme group for enhancing its fluorescence.

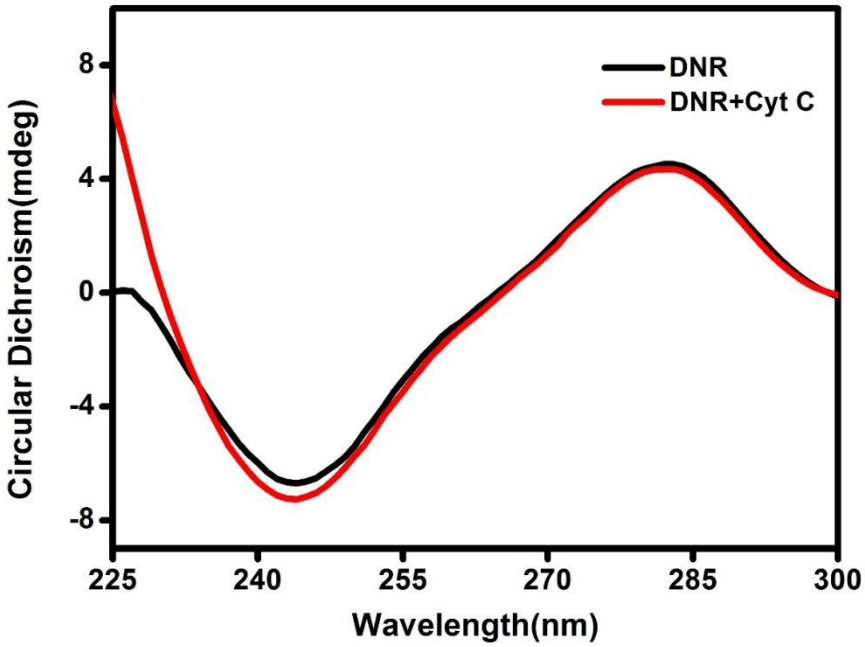

Fig. S13 CD spectra of DNR1 (black) and Cyt C+DNR1 (red). [Cyt C]=5 μM, [DNR1]=1 μM.

Fig. S13 show that the observed CD spectra of DNR1 consist of a positive band at 282 nm due to base stacking and a negative band at 248.4 nm due to helicity, which is characteristic of DNA in the right-handed B form. We observed the same band position and intensity in the presence of Cyt C at the 200–280 nm wavelength range suggesting that there is groove binding and electrostatic interaction between Cyt C and DNR1.